New single-phase, white light-emitting phosphors based on δ-$Gd_2Si_2O_7$ for solid state lighting

Alberto José Fernández-Carrión,[a,b] *Manuel Ocaña,*[a] *Jorge García-Sevillano*[c] *,*

Eugenio Cantelar,[c] *and Ana Isabel Becerro*[a,*]

[a]*Instituto de Ciencia de Materiales de Sevilla (CSIC-University of Seville). c/ Américo Vespucio, 49. 41092 Seville (Spain).*

[b]*Departamento de Química Inorgánica (Universidad de Sevilla). 41071 Seville (Spain).*

[c]*Dpto. Física de Materiales, C-04. Universidad Autónoma de Madrid, 28049 Madrid (Spain).*

*Corresponding author: e-mail address: anieto@icmse.csic.es. Tel no. +34 954489545, Fax no: +34 954460165

ABSTRACT

Two new white light (WL)-emitting phosphors (δ-$Gd_2Si_2O_7$:Dy and δ-$Gd_2Si_2O_7$:Eu,Tb) have been synthesized by the sol-gel method. The Gd-Ln^{3+} (Ln^{3+}= Dy^{3+}, Tb^{3+}, Eu^{3+}) energy transfer band has been used to excite both phosphors, which provides an enhancement of the Ln^{3+} emissions. Firstly, WL was generated from δ-$Gd_2Si_2O_7$:*x*Dy thanks to the particular ratio of the blue and yellow emissions observed in all three compositions, which showed chromatic coordinates *x*=0.30, *y*=0.33 and CCT values between 7077 K and 6721 K. The decay curves of the main transitions of Dy^{3+} showed a maximum lifetime value for δ-$Gd_2Si_2O_7$:0.5%Dy, which is, therefore, the most efficient doping level. Secondly, a broad spectral range, single-phase, WL-emitting phosphor was generated by co-doping δ-$Gd_2Si_2O_7$ with Tb^{3+} and Eu^{3+}. The composition δ-$Gd_2Si_2O_7$:0.3%Eu^{3+};0.8%Tb^{3+} showed CIE coordinates well inside the ideal WL region of the CIE diagram and a CCT value of 5828 K. The single-phase WL-emitting phosphors presented in this paper are promising materials to be used in white solid state lighting systems and field-emission displays due to both, the advantages provided by Gd^{3+} ions as well as by the high thermal and chemical stability of the rare earth disilicate matrix.

Keywords: rare earth silicates, luminescence, LEDs, energy transfer

1. INTRODUCTION

White Solid State Lighting (white SSL), based on LEDs, uses nowadays a mature technology that can compete with the traditional incandescent and fluorescent lamps.[1] It has numerous advantages over the latter such as small size, high lifetime, robustness, fast switching, efficiency, and energy saving. Basically two approaches can be followed to obtain a white SSL. On the one hand, the phosphor-free SSL, known as RGB-LEDs, consist of three or more LEDs with power ratios adjusted to obtain white light. The main disadvantage of this SSL approach is that a complex electronics have to be used due to the different driving currents required by the different color LEDs. On the other hand, a SSL device made of phosphor-converted LEDs, uses an ultraviolet (UV) LED in combination with several phosphors, which convert part of the UV light emitted by the LED into white light. Currently, most of the commercially available white SSL are based on this second approach. They were initially made from a blue emitting LED (InGaN) coated with a yellow phosphor (YAG:Ce^{3+}),[2] so that the combination of the blue and yellow lights generated WL. However, this type of SSL suffers from some weaknesses, such as poor color rendering index and low stability of color temperature.[3] On the other hand, SSL based on UV-LEDs coated with RGB tri-color phosphors show the disadvantage associated to the different velocity of degradation of each phosphor. White light (WL)-emitting single-phase phosphors might overcome the problems mentioned above and it is considered that they might be the direction of white SSL development.[4] There are different approaches to obtain WL-emission in a single-phase host, namely *i)* doping a single rare earth (RE) ion into the appropriate matrix, *ii)* co-doping various RE ions with different emissions into a single host which are then excited simultaneously, *iii)* co-doping different ions in one matrix and control the emission via energy transfer processes, and *iv)* controlling the concentration of the defect and reaction conditions of defect-related luminescent materials.[5]

An important performance requirement for WL-emitting phosphors is, among others, an excellent chemical and temperature stability. A number of phosphate-,[6,7,8] wolframate-,[9] oxide-,[10] vanadate-,[11] and borate-based WL-emitting phosphors have been proposed in the literature. However, in spite of the high chemical and thermal stability shown by rare earth (RE) silicates, only two reports have been found in the literature about phosphors based on these matrices, namely (Ce,Eu,Tb)-doped $Y_2Si_2O_7$[12] and (Ce,Tb)-doped $Lu_2Si_2O_7$.[13]

$Gd_2Si_2O_7$ is an inert matrix in the visible region of the electromagnetic spectrum and shows an additional advantage respect to $Y_2Si_2O_7$ and $LuSi_2O_7$, consisting in the well-known ability of Gd^{3+} ions to efficiently absorb UV radiation and transfer it to a number of active lanthanide ions like Dy^{3+}, Tb^{3+} and Eu^{3+}.[14] $Gd_2Si_2O_7$ exhibits two different polymorphic forms.[15] The low temperature polymorph, α-$Gd_2Si_2O_7$, consists of isolated chain-like (Si_3O_{10}) groups plus additional (SiO_4) tetrahedra, while the more simple δ-$Gd_2Si_2O_7$ structure contains all Si atoms arranged in (Si_2O_7) double-tetrahedra groups. The Gd^{3+} ions are located in 4 different crystallographic sites in the α-$Gd_2Si_2O_7$ unit cell, while only 2 Gd^{3+} sites are present in the unit cell of the δ-$Gd_2Si_2O_7$ polymorph (Figure 1). While there are several studies about the optoelectronic applications of the α-$Gd_2Si_2O_7$ matrix in the literature,[16,17] no report has been found on the use of δ-$Gd_2Si_2O_7$ as a matrix for the fabrication of phosphors. The latter fact, together with the simpler structure of the δ-polymorph has led us to use it in the present study.

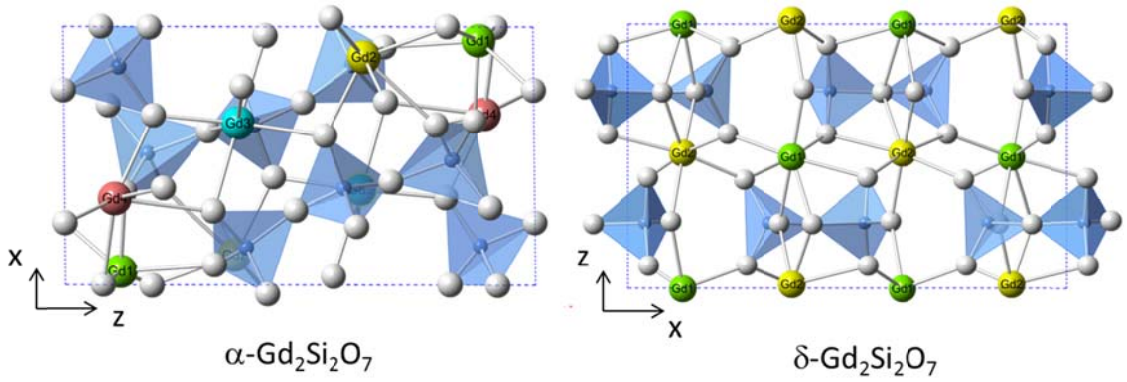

Figure 1: Crystal structure of the two polymorphic forms of $Gd_2Si_2O_7$. Left: Triclinic (*P-1*) α-form. Right: Orthorhombic (*Pna2₁*) δ-form.[15]

Herein we have used δ-$Gd_2Si_2O_7$ to fabricate two WL-emitting, single-phase phosphors of types *i)* and *ii)* described above. One of them is obtained after doping the matrix with Dy^{3+} ions. The Dy^{3+} ions are able to emit radiation in both, the blue and yellow regions after UV excitation. An adequate ratio of both emissions could result in the emission of WL. Such ratio depends on the crystal structure of the matrix as well as on its chemical composition,[18,19] and all these factors have been analyzed in this paper. Likewise, the decay curves of both emissions have been recorded for several Dy^{3+} contents aiming at formulating the most efficient phosphor. On the other hand, a broad spectral range white emission could be obtained after doping the $Gd_2Si_2O_7$ matrix with different lanthanide ions emitting in the blue, green and red regions of the spectrum after simultaneous

excitation through the Gd-Ln^{3+} energy transfer band. Based on the known capacity of Tb^{3+} to emit in both the blue and green regions in certain matrices and at specific doping levels, we have firstly analyzed this feature in single-doped $Gd_2Si_2O_7$:Tb. We have subsequently co-doped the matrix with different proportions of Tb^{3+} and Eu^{3+} ions, the latter as the source of the red emission, to find the composition that best fits the ideal WL emission. Finally, the dynamics of the luminescence of Tb^{3+} and Eu^{3+} ions have been analyzed in both the co-doped sample as well as in the corresponding single doped ones to determine the presence of any energy transfer process.

2. EXPERIMENTAL SECTION

2.1. Synthesis

δ-$Gd_2Si_2O_7$, δ-$Gd_2Si_2O_7$ singly doped with Dy^{3+} (0.5-2.0 molar %), Tb^{3+} (0.5-5 molar %) and Eu^{3+} (0.3-10 molar %), and δ-$Gd_2Si_2O_7$ codoped with different percentages of Tb^{3+} and Eu^{3+} were synthesized by a sol gel method using the following precursors: $Ln(NO_3)_3 \cdot 6H_2O$ (Ln= Gd^{3+}, Dy^{3+}, Tb^{3+} and Eu^{3+}) (99,99% Aldrich Chemical Co.), $Si(OC_2H_5)_4$ (TEOS, 99% Aldrich Chemical Co.), and CH_3CH_2OH (ethanol pure, Aldrich Chemical Co.). The standard procedure was as follows: A TEOS solution in ethanol (1:3 in volume) was added over the appropriate amounts of lanthanide nitrates previously dissolved in pure ethanol. A slight excess of TEOS (1.1:1 TEOS/$RE(NO_3)_3$ mol %) in the initial mixture was necessary to suppress formation of an undesired oxyorthosilicate phase. The mixture was stirred at 40 ºC until the formation of a transparent gel, which was then calcined at 60 ºC for 24 h in air. Finally, the samples were heated at 500 ºC for 2 h using a heating rate of 1 ºC min^{-1} to remove nitrate. The resulting powders were subsequently annealed at 1600 ºC for 48 h.

2.2. Characterization techniques

X-ray powder diffraction (XRD) data were recorded on a PANalytical X`Pert Pro Diffractometer (CuK_α) with an X-Celerator detector over an angular range of $10º < 2\theta < 120º$, 2θ step width of 0.016º. The ICDD powder diffraction database[20] was used to identify the crystalline phases in the powder patterns. Likewise, the XRD patterns were analysed using the TOPAS software[21] and the JEdit editor[22] to obtain the corresponding

unit cell volumes and prove the isomorphic substitution of Gd^{3+} for the different dopants (Dy^{3+}, Tb^{3+} and Eu^{3+}). Refined parameters were: background coefficients, zero error, scale factors, unit cell parameters, and atomic positions.

The excitation and emission spectra of the powder phosphors were recorded in a Horiba Jobin-Yvon Fluorolog3 spectrofluorometer operating in the front face mode. The CIE color coordinates of the emitted light were calculated from the emission spectra considering a 2º observer. The correlated color temperature (CCT) values of the white ligh-emitting phosphors were calculated from the corresponding color coordinates using the McCamy equation[23] ($CCT = -449n^3 + 3525n^2 - 6823n + 5520.33$, where $n = (x-x_e)/(y-y_e)$, where $x_e = 0.332$ and $y_e = 0.186$). The photoluminescence quantum yield (QY) of the optimum emitting Eu,Tb:δ-$Gd_2Si_2O_7$ and Dy:δ-$Gd_2Si_2O_7$ phosphors, defined as the ratio between photons emitted and absorbed by the powders, was determined by an absolute method upon excitation through the Gd^{3+}-Ln^{3+} energy transfer band at 312 nm. The measurements could not be done at 273 nm (the most intense Gd→Ln energy transfer band) because 300 nm was the fluorimeter limit for this type of measurement. Each measurement was repeated several times and the average value obtained was reported. The set up used consisted of an integrating sphere (Labsphere) with its inner face coated with Spectralon, attached to the spectrofluorimeter. A Spectralon block situated in the sample holder was used as a blank. Spectral correction curves for sphere and emission detector were provided by Horiba Jobin-Yvon. Lifetime measurements were obtained under pulsed excitation at 355 nm and 532 nm, depending on the active lanthanide analysed, by using the second and third harmonics, respectively, of a Nd:YAG laser (Spectra Physics model DCR 2/2A 3378) with a pulse width of 10 ns and a repetition rate of 10 Hz. The fluorescence was analyzed through a Princeton Instruments monochromator (Acton SP2500) and then detected synchronously with an EMI-9558QB photomultiplier and recorded by a Tektronix TDS420 digital oscilloscope.

3. RESULTS

3.1. WL generation from Dy-doped δ-$Gd_2Si_2O_7$ phosphors

3.1.1. Crystal structure of Dy-doped δ-$Gd_2Si_2O_7$

The XRD patterns of the 0.5, 1.0 and 2.0% Dy-doped δ-$Gd_2Si_2O_7$ samples (Figure S1) showed, exclusively, reflections corresponding to δ-$Gd_2Si_2O_7$ (PDF 00-024-0065), which proves the purity of the samples. All XRD patterns were apparently very similar to each other, with no changes in intensity or line positions in spite of the fact that the samples were doped with Dy^{3+}. This fact could be due to both the low Dy contents used for the doping as well as to the similar X-ray scattering factors of Gd^{3+} and Dy^{3+}. To prove the isomorphic substitution of Gd^{3+} for Dy^{3+} the XRD pattern of the undoped and the 2% Dy-doped samples were analyzed using the Rietveld method. Starting parameters were taken from those reported by Smolin and Shepelev[24] for δ-$Gd_2Si_2O_7$, which consider an orthorhombic cell with space group *Pna2₁*, where Gd ions are located in sites without inversion centres. Figure 2 shows the experimental and fitted patterns for the 2% Dy-doped samples. It can be observed that all reflections could be fitted on the basis of the *Pna2₁* orthorhombic cell. Unit cell volumes obtained were 581.48(1) and 581.33(1) for the undoped and doped samples, respectively, which is compatible with the smaller ionic radius of Dy^{3+} compared to Gd^{3+}.[25] The synthesis procedure allows, therefore, the isomorphic substitution of Gd^{3+} for Dy^{3+} and renders a single phase.

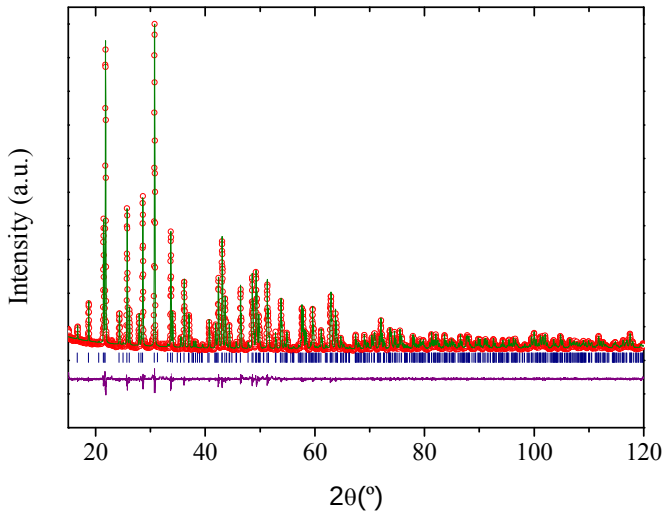

Figure 2: Experimental (crosses) and fitted (lines) powder X-ray diffraction pattern of 2% Dy^{3+}-doped δ-$Gd_2Si_2O_7$. The difference curve is also included.

3.1.2. Luminescence properties of Dy-doped δ-$Gd_2Si_2O_7$

The excitation spectrum recorded on the δ-$Gd_2Si_2O_7$:1%Dy^{3+} sample by monitoring the Dy^{3+} emission at 476 nm (Figure 3a) displayed strong bands at 273 nm and 312 nm along with much weaker features in the 320-400 nm range. The latter are due to the

direct excitation of the Dy^{3+} ground state to higher levels of the 4f-manifold, whereas the former can be ascribed to the electronic transitions from the ground state level of Gd^{3+} ($^8S_{7/2}$) to the $^6I_{11/2}$ and ^6P_J excited levels, respectively.[26] This indicates that an energy transfer from Gd^{3+} multiplets to Dy^{3+} electronic levels takes place in this sample. The excitation spectra of the rest of Dy-doped samples were very similar to the one of Figure 3a.

The emission spectrum of the δ-$Gd_2Si_2O_7$:1%Dy^{3+} sample, recorded after exciting through the Gd→Dy energy transfer band at 273 nm (Figure 2b), was very similar to that obtained after direct excitation of the Dy^{3+} electronic levels (λ_{exc} = 350 nm), also shown in Figure 3b, although their intensities were extremely different, as expected from Figure 3a. The use of a Gd-based matrix allowed, therefore, increasing the

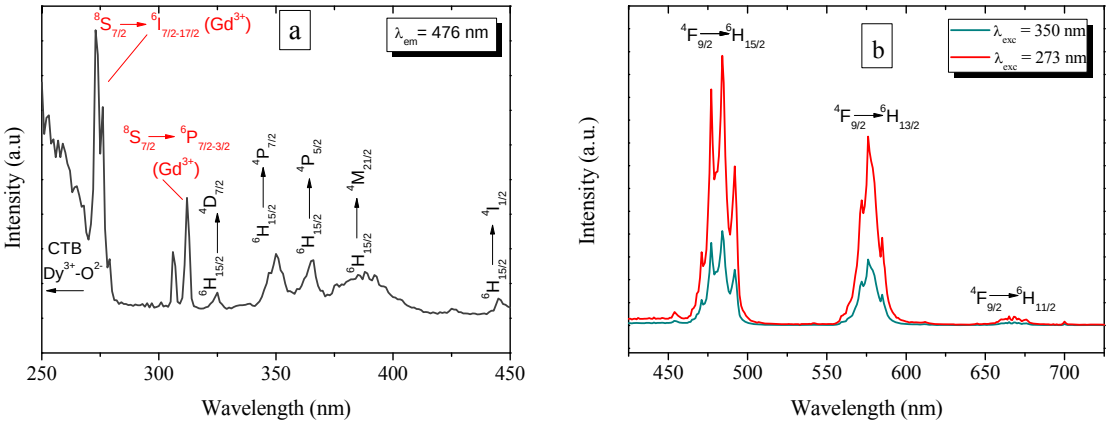

Figure 3: Excitation (λ_{em}= 476 nm) (*a)* and emission (*b)* spectra of 1% Dy^{3+}-doped δ-$Gd_2Si_2O_7$. The emission spectra were recorded at 273 nm and 350 nm

efficiency of the phosphor.

The spectra of the two other compositions were very similar to these ones and are not shown. The emission spectra showed two dominant bands in the blue (460-500 nm) and yellow (550-600 nm) regions. The yellow emission, corresponding to the $^4F_{9/2} \rightarrow {}^6H_{13/2}$ transition, is a forced electric dipole transition, hypersensitive to the site symmetry of the Dy^{3+} ions, so that it is only allowed at low symmetries with no inversion center.[27] The fact that this transition was clearly observed in our spectra indicates that Dy^{3+} is located at a site without inversion center, as expected from the replacement of Gd^{3+} in the *4a* sites of the *Pna2₁* structure, as described above. On the other hand, in those cases where the $^4F_{9/2} \rightarrow {}^6H_{13/2}$ transition is allowed by the forced electric dipole mechanism,

as it is our case, its intensity is normally greater than that of $^4F_{9/2} \rightarrow {}^6H_{15/2}$,[28] but this is not our case, as the ($^4F_{9/2} \rightarrow {}^6H_{13/2}$)/($^4F_{9/2} \rightarrow {}^6H_{15/2}$) or Y/B (Yellow/Blue) ratio = 0.74, 0.72 and 0.79 for the 0.5, 1.0 and 2% Dy-doped samples, respectively. A Y/B ratio lower than 1 has also been observed for other crystalline Dy-doped samples with Dy at non-centrosymmetric sites[29,30] and has been assigned to the influence of other factors like the electronegativity of the next-nearest neighbors, which influences the covalency of the Dy-O bond.[31]

The Y/B ratio observed for the δ-$Gd_2Si_2O_7$:Dy^{3+} phosphors analyzed in this study resulted very adequate for the generation of white light. The color coordinates were x=0.30, y=0.33 for the three compositions analyzed, which fall well inside the ideal white light region of the CIE diagram.[32] The CCT values, calculated using the empiric formula given by McCamy[23] were 7077 K, 7111 K, and 6721 K for the 0.5, 1.0 and 2% Dy doped samples, respectively. This temperature is some 1000 K higher than the highest CCT reported in the literature for Dy^{3+}-based phosphors,[33,34,35] which makes this phosphor very useful for inside illumination of offices, classrooms, etc., where a cold lighting (higher CCT) is used to enhance concentration.[36]

3.1.3. Luminescence dynamics: Lifetimes and optimum Dy content

Although the emission spectra of the three δ-$Gd_2Si_2O_7$:$x$$Dy^{3+}$ compositions were very similar to each other and, consequently, all three phosphors emitted white light after UV excitation, it is important to determine the optimum Dy content to formulate the most efficient composition. With this purpose we registered the decay curves of the $^4F_{9/2} \rightarrow {}^6H_{15/2}$ and $^4F_{9/2} \rightarrow {}^6H_{13/2}$ transitions under pulsed excitation using the third harmonics of a Nd:YAG laser at λ_{exc} = 355 nm. Under this excitation, the $^4P_{7/2}$ multiplet is directly populated and a non-radiative relaxation mechanism populates the $^4F_{9/2}$ state (Figure 4, left). Radiative relaxation of this state produces an emission spectrum like that of Figure 3b. The decay curves of the blue and yellow emissions were coincident and those corresponding to the $^4F_{9/2} \rightarrow {}^6H_{15/2}$ have been plotted in Figure 4 (right) for the three Dy contents. The decays were correctly fitted by using a biexponential temporal dependence

$$I(t) = I_{01}\exp(-t/\tau_1) + I_{02}\exp(-t/\tau_2) \qquad (1)$$

where *I(t)* is the luminescence intensity, *t* is the time after excitation, and τ_i (i = 1,2) is the decay time of the ith component, with intensity I_{0i}. The average decay times, $\langle\tau\rangle$, calculated as

$$\langle\tau\rangle = \frac{\int_0^\infty tI(t)dt}{\int_0^\infty I(t)dt} = \left(\tau_1^2 I_{01} + \tau_2^2 I_{02}\right)/\left(\tau_1 I_{01} + \tau_2 I_{02}\right) \qquad (2)$$

have been plotted in the inset of Figure 4(right). The maximum <τ> value (1.45 ms) corresponded to the sample with 0.5% Dy. The average lifetime decreased slightly when increasing the Dy content to 1.0%, and then it dropped drastically to 0.84 ms at 2.0% Dy. This fact is due to a concentration quenching effect produced by the increase in the number of emitter centres. It can be therefore concluded that the optimum Dy doping level of the studied δ-$Gd_2Si_2O_7$ samples is 0.5%. This low value is in agreement with previous studies on other Dy-doped systems such as aluminates,[37] zincates,[38] and phosphates.[6,39] The quantum yield of the 0.5%Dy-doped sample was found to be 15(6)% at 312 nm

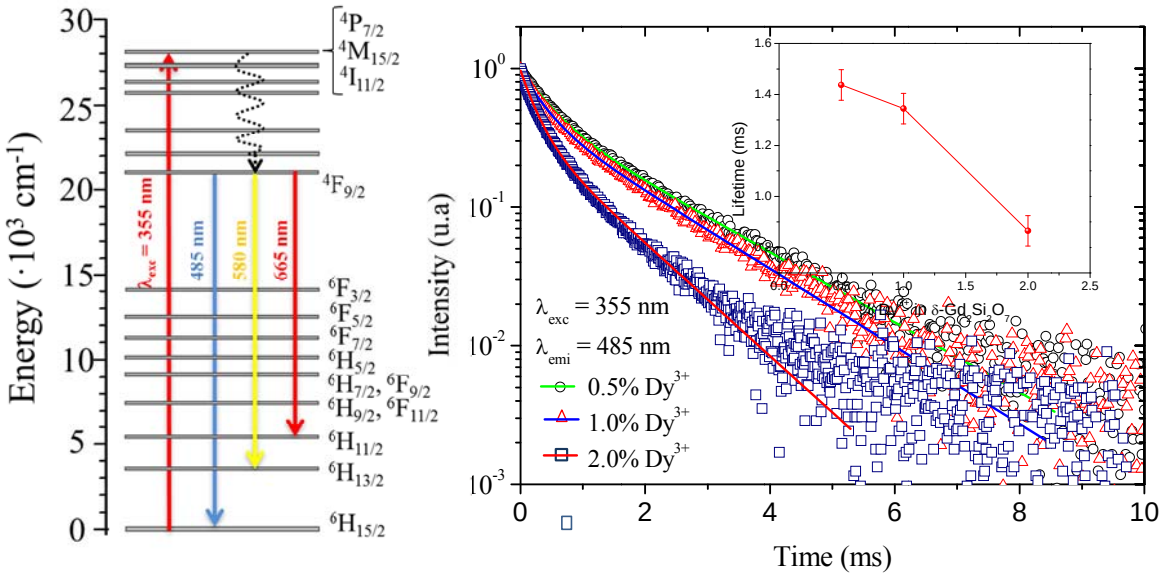

excitation.

Figure 4: Left: Energy level diagram of Dy^{3+} ions showing the relevant luminescent emissions. Under 355 nm (pulsed) excitation the $^4F_{9/2}$ level is populated, giving rise to emissions in the 450-725 nm wavelength range. Right: Decay curves of the $^4F_{9/2}\rightarrow{}^6H_{15/2}$ (485 nm) transition of Dy^{3+} in the δ-$Gd_2Si_2O_7$:Dy^{3+} phosphors, recorded after excitation at 355 nm. The inset is a plot of the lifetime values versus Dy^{3+} content for the $^4F_{9/2}\rightarrow{}^6H_{15/2}$ (485 nm) transition.

3.2. WL generation from Eu,Tb-co-doped δ-$Gd_2Si_2O_7$ phosphors

Although the above described phosphor emits light in the ideal white light region of the CIE diagram with a singular CCT, it lacks the red component, which could lead to a poor Color Rendering Index (CRI).[40,41] In order to synthesize a single-phase phosphor, which emits white light with broad spectral dispersion, we have codoped the δ-$Gd_2Si_2O_7$ matrix with Tb^{3+} and Eu^{3+}. The reasons to use these two active lanthanides as dopants are the following. *i)* It is well known that Gd^{3+} efficiently absorbs UV radiation and also efficiently transfers it to several active lanthanide ions like Eu^{3+} and Tb^{3+}.[14] Therefore, both lanthanides can simultaneously be excited through the Gd-Ln energy transfer band. *ii)* Likewise, Tb^{3+} in low concentrations is able to emit not only green but also blue light after excitation with UV radiation,[42,43,44,45] although this emission is not a common feature of all matrices.[46,47] A single-phase white-light-emitting δ-$Gd_2Si_2O_7$ phosphor could, therefore, be synthesized, if the latter emission is confirmed for Tb-doped δ-$Gd_2Si_2O_7$, by combining the red emission from Eu^{3+} with the green and blue emissions from Tb^{3+} by using the appropriate doping concentrations of both ions.

3.2.1. Luminescent properties of Tb-doped δ-$Gd_2Si_2O_7$ phosphors

In order to check that δ-$Gd_2Si_2O_7$:$x$$Tb^{3+}$ phosphors are able to emit in the blue region at low Tb contents, we have firstly synthesized different samples with Tb contents from 0.5 to 5 molar %. Figure S2 shows the corresponding XRD patterns, which consist of reflections matching PDF 00-024-0065, corresponding to δ-$Gd_2Si_2O_7$. All patterns were very similar to each other due to both, the low doping levels as well as the similar Gd^{3+} and Tb^{3+} ionic radii[25] and X-ray scattering factors. As a consequence of these

circumstances, only a very slight decrease was observed in the unit cell volume (calculated using the Rietveld method) from 582.23(1) $Å^3$ in the undoped material to 582.08(2) $Å^3$ in the 5% Tb doped sample, which demonstrates the effective substitution of Gd for Tb in the δ-$Gd_2Si_2O_7$ structure.

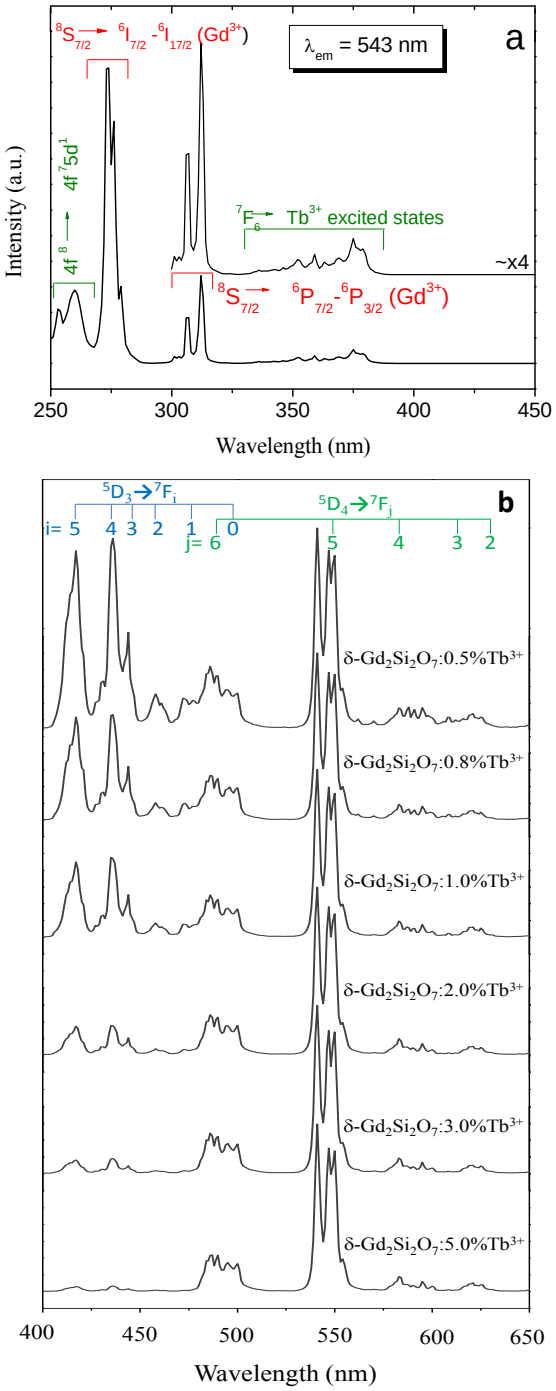

Figure 5: *a)* Excitation spectrum of the δ-$Gd_2Si_2O_7$:1%Tb phosphor monitoring the characteristic 543 nm emission of Tb^{3+}. *b)* Emission spectra of δ-$Gd_2Si_2O_7$:$x$$Tb^{3+}$ phosphors recorded after excitation at 273 nm.

Figure 5a shows the excitation spectrum of δ-$Gd_2Si_2O_7$:1%Tb^{3+} registered while monitoring the emission characteristic of Tb^{3+} at 543 nm. The spectra corresponding to the rest of compositions were qualitatively very similar to this one. They consist of a set of low intensity bands in the 325-400 nm region corresponding to the direct excitation of the Tb^{3+} ground state ($^7F_6$) to higher levels of the 4f-manifold ($^5D_{4\text{-}0}$, $^5G_{6\text{-}2}$, $^5L_{4\text{-}0}$, and $^5H_7$)[48]. The high intensity, narrow lines in the 270-325 nm can be ascribed to the electronic transitions from the ground state level of Gd^{3+} ($^8S_{7/2}$) to its $^6I_{11/2}$ and ^6P_J excited levels.[48] The observation of Gd absorption bands in this spectrum, where the emission of Tb^{3+} is being monitored, proves the energy transfer from Gd^{3+}multiplets to Tb^{3+} electronic levels in this sample. Finally, the high energy bands (253 nm and 260 nm) are due to the parity allowed $4f^8 \rightarrow 4f^7 5d^1$ transitions of Tb^{3+}.[12,49,50] The emission spectra of the δ-$Gd_2Si_2O_7$:x%Tb^{3+} samples (x=0.5-5.0), registered at λ_{exc}= 273 nm (Gd→Tb energy transfer band) have been plotted in Figure 5b, normalized to the intensity of the 543 nm band. The bands in the blue region of the spectrum (400-475 nm) are mainly due to $^5D_3 \rightarrow {}^7F_i$ (i = 0, 1, 2, 3, 4, 5) transitions while the $^5D_4 \rightarrow {}^7F_i$ (i = 2, 3, 4, 5, 6) transitions are observed as emission bands in the green region (480-630 nm). It can be observed that the intensity of the blue emission is prominent at very low Tb contents and it decreases with increasing Tb content, becoming eventually very low at Tb contents >1%. This phenomenon can be explained by the cross-relaxation effect: The energy difference between $^5D_3$ and $^5D_4$ levels (5600 cm^{-1}) in Tb^{3+} is basically equal to that between $^7F_0$ and $^7F_6$ (5800 cm^{-1}).

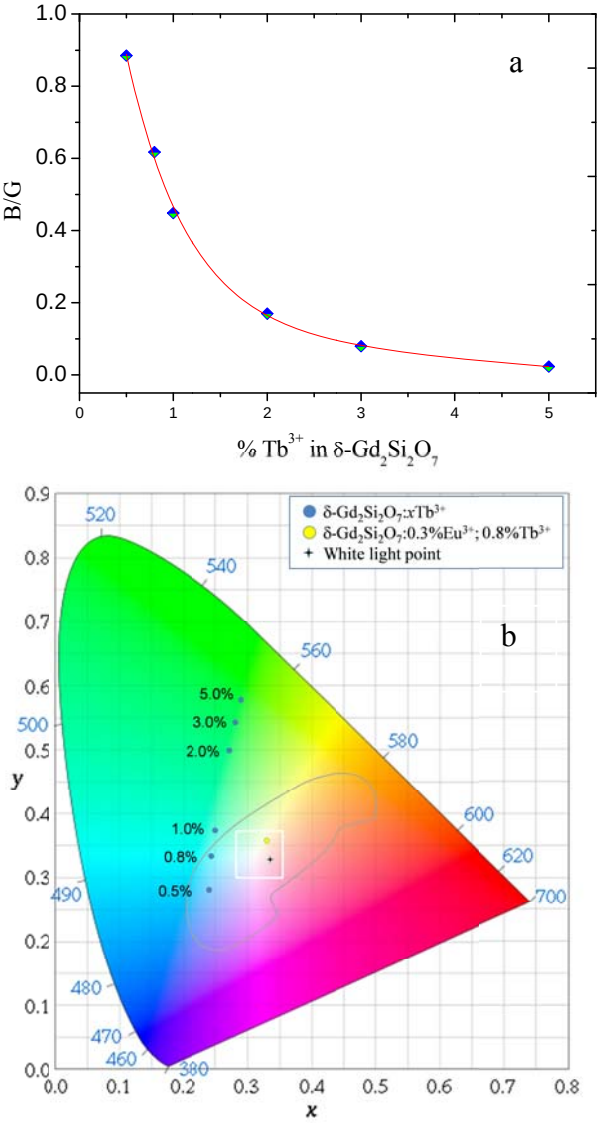

Figure 6: *a)* Blue/Green emission intensity ratio as a function of Tb content in δ-$Gd_2Si_2O_7$. *b)* CIE diagram with the chromatic coordinates of δ-$Gd_2Si_2O_7$:*x*Tb^{3+} (blue circles), δ-$Gd_2Si_2O_7$:0.3Eu^{3+}; 0.8Tb^{3+} (yellow circle), and white light point (cross).

This fact allows a resonant phenomenon between the relaxation from $^5D_3$ to $^5D_4$ in one Tb^{3+} ion and the excitation from $^7F_6$ to $^7F_0$ in the neighboring Tb^{3+}.[14] This process takes place only when two Tb^{3+} ions are close enough to each other, that is, when the Tb concentration reaches a certain value. An exponential decrease of the Blue/Green (B/G) intensity ratio with Tb content is observed in Figure 6a, which suggests that the quenching concentration of the blue emission could be located at Tb contents even lower than 0.5%. A similar dependence of the B/G intensity ratio with Tb content was reported for $Y_3Al_{5-x}Ga_xO_{12}:Tb^{3+}$.[42] In summary, it is possible to tune the chromaticity of the Tb^{3+} emission by changing the doping level from 0.5 to 5.0%. The change in chromaticity from blue to green can be observed in the CIE diagram plotted Figure 6b.

3.2.2. Luminescence properties of Eu^{3+},Tb^{3+} co-doped δ-$Gd_2Si_2O_7$ phosphors.

Once demonstrated that δ-$Gd_2Si_2O_7$ doped with Tb^{3+} levels < 1% produces emission in both the blue and green regions of the spectrum, we have co-doped the δ-$Gd_2Si_2O_7$ matrix with Tb^{3+} and Eu^{3+}, varying systematically the Eu and Tb concentrations and keeping always the Tb content below 1 molar %. The XRD patterns of all the samples (Figure S3) showed only reflections corresponding to δ-$Gd_2Si_2O_7$, which proves the purity of the phase, and the reflections were very slightly shifted due to the replacement of Gd^{3+} for Tb^{3+} and Eu^{3+} in the unit cell.

Figure 7 shows, as an example, the emission spectra of two of the compositions synthesized, namely, δ-$Gd_2Si_2O_7$:0.7%Eu^{3+};0.8%Tb^{3+} and δ-$Gd_2Si_2O_7$:0.3%Eu^{3+}; 0.8%Tb^{3+}, recorded after excitation through the Gd-Ln energy transfer band (λ_{exc}= 273 nm). Both spectra show emission across the whole visible range of the spectra, that is, in the blue, green and red regions. This is due to the simultaneous excitation of both Tb^{3+} and Eu^{3+} at 273 nm, as well as to the low concentration of Tb, which allows observation of the blue emission, as explained above. Both spectra show, however, different relative intensities of the Tb and Eu bands due to the different Eu/Tb contents of the samples. Thus, the higher the Eu content, the higher the intensity of the bands in the 525-725 nm range, which are characteristic of this ion. It is important to note that the spectra of the co-doped samples do not match with the sum of the spectra of the corresponding single-doped samples. This is likely due to the existence of energy transfer phenomena between the two dopants, which will be analyzed later in this paper.

Among the large set of compositions synthesized the δ-$Gd_2Si_2O_7$:0.3%Eu^{3+}; 0.8%Tb^{3+} sample showed the CIE coordinates (yellow circle in Figure 6b) closest to the WL point (x=0.33, y=0.33). The CCT of this new single-phase, WL phosphor, calculated using the McCamy equation,[23] was 5828 K, which is a warmer white than that emitted by the Dy-doped δ-$Gd_2Si_2O_7$ phosphor described above. In addition, the fact that the WL emitted by this phosphor is of broad spectral range (blue, green and red components), will contribute to a high color rendering index. The quantum yield of the δ-$Gd_2Si_2O_7$:0.3%Eu^{3+}; 0.8%Tb^{3+} was found to be 41(12)% at 312 nm excitation.

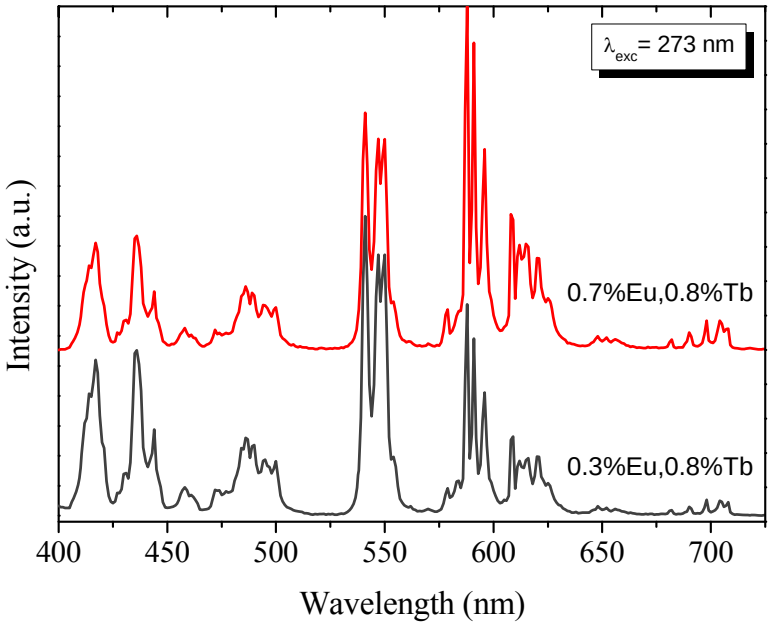

Figure 7: Emission spectra of co-doped δ-$Gd_2Si_2O_7$:Eu^{3+},Tb^{3+} phosphors with different Eu and Tb contents, recorded after excitation at 273 nm.

3.2.3. Tb^{3+}→ Eu^{3+} energy transfer

Energy transfer processes between Tb^{3+} and Eu^{3+} have been reported in the literature for several matrices co-doped with both ions.[51,52,53,54,55] To check the existence of such phenomenon in our WL-emitting phosphor, we have studied the luminescence dynamics under pulsed laser excitation in the co-doped as well as in the corresponding single doped materials, that is, δ-$Gd_2Si_2O_7$:0.3%Eu^{3+};0.8%Tb^{3+}, δ-$Gd_2Si_2O_7$:0.3%Eu^{3+} and δ-$Gd_2Si_2O_7$:0.8%Tb^{3+} under pulsed excitation using the second and third harmonics of a Nd:YAG laser at λ_{exc} 532 nm and 355 nm, respectively. The use of one or the other λ_{exc} depended on the specific objective and will be explained in each case.

Tb^{3+} decay curves: Figures 8a and 8b show the decay curves corresponding to the 435 nm ($^5D_3 \rightarrow {}^7F_4$) and 550 nm ($^5D_4 \rightarrow {}^7F_5$) emissions of Tb^{3+}, respectively, for both the single doped (δ-$Gd_2Si_2O_7$:0.8%Tb^{3+}) and the codoped (δ-$Gd_2Si_2O_7$:0.3%Eu^{3+},0.8%Tb^{3+}) phosphors, under a λ_{exc}=355 nm. The emission spectra of the singly- and co-doped phosphors, recorded after excitation at 355 nm (Figure S4), are very similar to those obtained with λ_{exc}= 273 nm (Figures 5b and 7, respectively). The excitation with λ_{exc}=355 nm populates the $^5D_3$ levels of Tb^{3+} through a non-radiative decay from higher energy levels, while the $^5D_4$ states are likewise populated through a non-radiative decay from $^5D_3$ (Figure 9, left). While the 435 nm decay curves exhibit an exponential decay from the beginning, the 550 nm luminescence temporal evolution reveals an initial rise, reaching a maximum value and then an exponential decay. The observed rise is related to the fact that the emitting $^5D_4$ level becomes populated from the upper $^5D_3$ level and therefore its filling is expected to follow the dynamics of the blue-emitting level (Figure 9, left diagram).

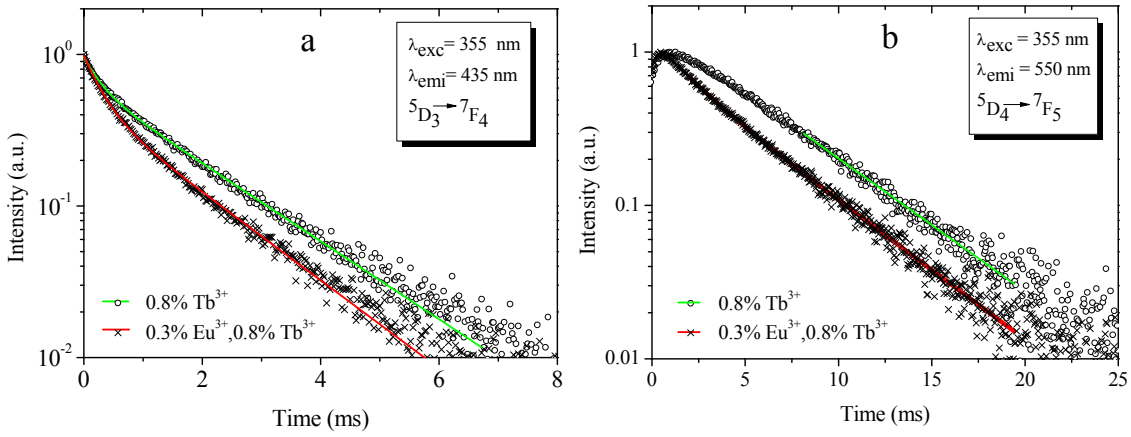

Figure 8: Experimental (symbols) and fitted (lines) decay curves of Tb^{3+} monitoring the $^5D_3 \rightarrow {}^7F_4$ (435 nm) emission *(a)* and the $^5D_4 \rightarrow {}^7F_4$ (550 nm) emission *(b)* for the δ-$Gd_2Si_2O_7$:0.8%Tb and δ-$Gd_2Si_2O_7$:0.3%Eu,0.8%Tb phosphors under excitation at 355 nm.

The decay curves were fitted to different types of exponential decays to eventually calculate lifetimes. On the one hand, the 435 nm decay curves could be described by a double-exponential dependence like that given above by equation (1), and the average lifetime values were then calculated using equation (2). The results are given in Table 1 for both the singly-doped and co-doped samples. On the other hand, the 550 nm decay

curve of the singly-doped sample could be described with a single exponential dependence given by equation (3)

$$I(t) = I_{01}\exp(-t/\tau_1) \qquad (3)$$

where *I(t)* is the luminescence intensity, *t* is the time after excitation, and τ_1 is the decay time. The first portion of the curve, corresponding to the rise, was discarded for the fit. Finally, it was necessary to use a bi-exponential dependence like that of equation (1) to fit the 550 nm decay curve of the co-doped sample. The calculated lifetime values for

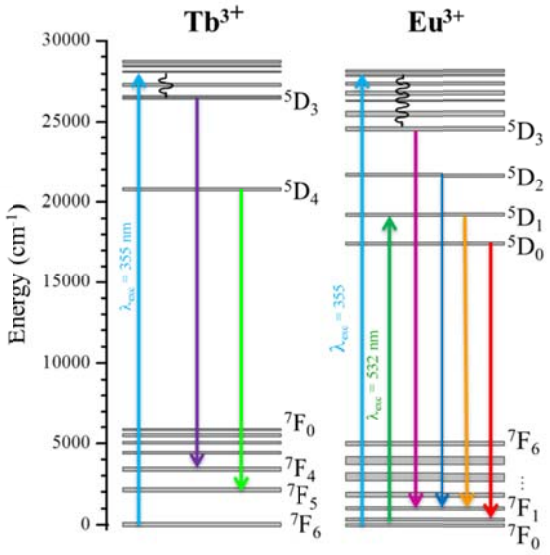

Figure 9: Energy level diagrams of Tb^{3+} and Eu^{3+} ions showing the relevant luminescent emissions. Under 355 nm (pulsed) excitation, the high energy level of both Tb^{3+} and Eu^{3+} ions are populated while only the high energy levels of Eu^{3+} are populated under 532 nm (pulsed) excitation.

both samples are given in Table 1. Those values, which are significantly lower for the co-doped sample, suggest that an energy transfer process from Tb^{3+} to Eu^{3+} ions takes place in the co-doped phosphor. This process is possible because the energy of the $^5D_3$ state of Tb^{3+} is very similar to that of the $^5G_2$ of Eu^{3+}.[52]

Table 1: Fitting parameters of the exponential temporal dependence for the luminescence decay curves of the Tb^{3+}-doped and Tb^{3+},Eu^{3+}-co-doped δ-$Gd_2Si_2O_7$ phosphors recorded at the blue (435 nm) and green (550 nm) emissions of Tb^{3+} ions.

	$^5D_3 \rightarrow {}^7F_4$ (435 nm)			$^5D_4 \rightarrow {}^7F_5$ (550 nm)		
δ-$Gd_2Si_2O_7$	τ_1 **(ms)**	τ_2 **(ms)**	$<\tau>$ **(ms)**	τ_1 **(ms)**	τ_2 **(ms)**	$<\tau>$ **(ms)**
0.8%Tb^{3+}	0.28 (34%)	1.69 (66%)	**1.57**	5.00	---	**5.00**

0.3%Eu^{3+}/0.8%Tb^{3+}	0.30 (52%)	1.49 (48%)	**1.28**	1.68 (39%)	4.80 (87%)	**4.40**

Eu^{3+} decay curves: The analysis of the Tb^{3+} decay curves described above revealed the existence of an energy transfer process from Tb^{3+} to Eu^{3+}. To determine the existence of an energy transfer process in the opposite sense, we have recorded the decay curves corresponding to the $^5D_0$-$^7F_1$ transition of Eu^{3+} (588 nm) in both the singly-doped (δ-$Gd_2Si_2O_7$:0.3%Eu^{3+}) and the co-doped (δ-$Gd_2Si_2O_7$:0.3%Eu^{3+},0.8%Tb^{3+}) phosphors under a λ_{exc}=532 nm (Figure 10). This energy directly populates the $^5D_1$ levels of Eu^{3+} while the $^5D_0$ states are likewise populated through a non-radiative decay from $^5D_1$ (Figure 9, right diagram). Likewise, the excitation energy of 532 nm is not able to excite the Tb^{3+} ions (as schematized in Figure 9, left) thus avoiding the overlap of Tb^{3+} and Eu^{3+} emissions of the co-doped phosphor in the 575-650 nm range (Figure S5), and allowing the analysis of the Eu^{3+} decay curves. Both decay curves of Figure 10 could be described by a double-exponential dependence like that given by equation (1), and the average lifetime values were then calculated using equation (2). The results are given in Table 2 for both the singly-doped and co-doped samples. The average lifetime values are very similar for both phosphors, the slight differences (lower than 5%) being due to the experimental error. These results suggest, therefore, that no energy transfer from Eu^{3+} to Tb^{3+} takes place in the co-doped sample under this excitation scheme.

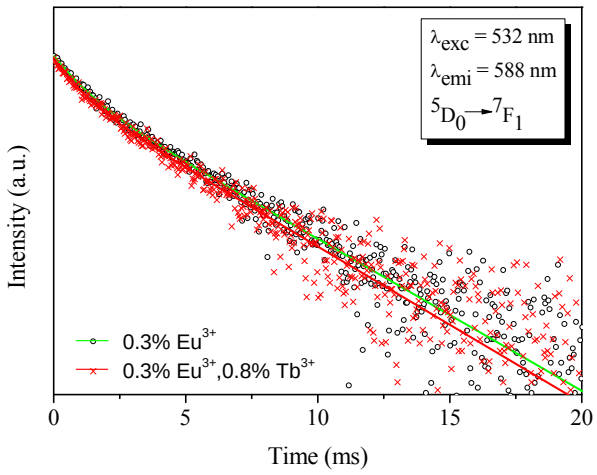

Figure 10: Experimental (symbols) and fitted (lines) decay curves of Eu^{3+} monitoring the $^5D_0 \rightarrow {}^7F_1$ (588 nm) emission in the δ-$Gd_2Si_2O_7$:0.3%Eu and δ-$Gd_2Si_2O_7$:0.3%Eu^{3+},0.8%Tb^{3+} phosphors under excitation at 532 nm.

Table 2: Fitting parameters of the bi-exponential temporal dependence for the luminescence decay curves of the Eu^{3+}-doped and Tb^{3+},Eu^{3+}-co-doped δ-$Gd_2Si_2O_7$ phosphors recorded at the 588 nm emission of Eu^{3+} ions.

$^5D_0 \rightarrow {}^7F_1$ (588 nm)			
δ-$Gd_2Si_2O_7$	τ_1 (ms)	τ_2 (ms)	$<\tau>$ (ms)
0.3% Eu^{3+}	1.10 (35%)	4.81 (65%)	4.4
0.3%Eu^{3+}/0.8%Tb^{3+}	1.01 (34%)	4.67 (66%)	4.3

4. CONCLUSIONS

We have fabricated two different single-phase, WL-emitting phosphors based on δ-$Gd_2Si_2O_7$. Firstly, doping the matrix with Dy^{3+} ions in the 0.5-2% range led to color coordinates (x = 0.30; y = 0.33) which lie well inside the ideal white light region of the CIE diagram. The optimum Dy^{3+} content, calculated from the corresponding decay curves, was found to be 0.5%, and the correlated color temperature (CCT) of this latter phosphor was 7077 K. Secondly, we have demonstrated that the chromaticity of δ-$Gd_2Si_2O_7$:Tb phosphors can be easily tuned from blue to green by changing the Tb concentration from 0.5% to 5%. This fact has then been exploited to fabricate a second single-phase, WL-emitting phosphor consisting of a δ-$Gd_2Si_2O_7$ matrix co-doped with 0.8% Tb^{3+} and 0.3% Eu^{3+}, the latter ion contributing with the red component necessary to produce white light. The resulting phosphor exhibited a luminescence well inside the ideal white light region (x = 0.32; y = 0.36) with a CCT of 5828 K. Finally, the analysis of the Tb^{3+} and Eu^{3+} decay curves has allowed establishing the existence of an energy transfer process from Tb^{3+} to Eu^{3+}. The two δ-$Gd_2Si_2O_7$-based phosphors described in this study present several advantages consisting, basically, in *i)* their high thermal and chemical stability, inherent to the rare earth disilicate family and *ii)* the enhancement of the emission intensity due to the Gd → Ln^{3+} energy transfer band. In addition, the CCT value of the phosphor can be tuned from warm to cold by changing the nature of the dopant ions (Dy or Tb+Eu), which could be interesting for the different applications of the white SSL devices.

ASSOCIATED CONTENT

Supporting Information:

- XRD patterns of the Dy-, Tb- and (Tb-Eu)-doped δ-$Gd_2Si_2O_7$ samples.

- Emission spectra of the δ-$Gd_2Si_2O_7$:0.3%Eu^{3+};0.8%Tb^{3+} and δ-$Gd_2Si_2O_7$:0.8%Tb^{3+} phosphors, recorded after pulsed excitation at 355 nm.

- Emission spectra of the δ-$Gd_2Si_2O_7$:0.3%Eu^{3+};0.8%Tb^{3+}, δ-$Gd_2Si_2O_7$:0.8%Tb^{3+} and δ-$Gd_2Si_2O_7$:0.3%Eu^{3+} phosphors, recorded after pulsed excitation at 532 nm.

This material is available free of charge via the internet at http://pubs.acs.org

AUTHOR INFORMATION

Corresponding author:

e-mail address: anieto@icmse.csic.es. Tel no. +34 954489545, Fax no: +34 954460165

Note:

The authors declare no competing financial interest.

ACKOWLEDGMENTS

A.J. Fernández-Carrión gratefully acknowledges an F.P.D.I. grant from Junta de Andalucía. Supported by MEC (Project. MAT2011-23593 and MAT2012-34919-SONAMFIBIOS), Junta de Andalucía (JA FQM 06090) and CSIC (201460E005).

REFERENCES

(1) Narukawa, Y.; Ichikawa, M.; Sanga, D.; Sano, M.; Mukai, T. White Light Emitting Diodes with Super-High Luminous Efficacy. *J. Phys. D: Appl. Phys.* **2010**, *43*, 354002.

(2) Fasol, G.; Nakamura S. The Blue Laser Diode: GaN Based Blue Light Emitters and Lasers, Springer, Berlin, 1997.

(3) Sheu, J. K.; Chang, S. J.; Kuo, C. H.; Su, Y. K.; Wu, L. W.; Lin, Y. C.; Lai, W. C.; Tsai, J. M.; Chi, G. C.; Wu, R. K. White-Light Emission from Near UV InGaN-GaN LED Chip Precoated with Blue/Green/Red Phosphors. *IEEE Photonic Tech. Lett.* **2003**, *15*, 18-20.

(4) Ye, S.; Xiao, F.; Pan, Y. X.; Ma, Y. Y.; Zhang, Q. Y. Phosphors in Phosphor-Converted White Light-Emitting Diodes: Recent Advances in Materials, Techniques and Properties. *Mater. Sci. Eng. R*. **2010**, *71*, 1-34.

(5) Shang, M.; Li, C.; Lin, How to Produce White Light in a Single-Phase Host. *J. Chem. Soc. Rev*. **2014**, *43*, 1372-86.

(6) Becerro, A. I.; Rodriguez-Liviano, S.; Fernández-Carrión, A. J.; Ocaña, M. A Novel 3D Architecture of $GdPO_4$ Nanophosphors: Multicolored and White Light Emission. *Cryst. Growth Des.* **2013**, *13*, 526−535.

(7) Liu, W. R.; Huang, C. H.; Yeh, C. W.; Chiu, Y. C.; Yeh, Y. T.; Liu, R. S. Single-Phased White-Light-Emitting $KCaGd(PO_4)_2:Eu^{2+},Tb^{3+},Mn^{2+}$ Phosphors for LED applications. *RSC Adv.* **2013**, *3*, 9023-9028.

(8) Zhang. J. C.; Long, Y. Z.; Zhang, H. D.; Bin, S.; Han, W. P.; Sun X. Y. Eu^{2+}/Eu^{3+}-Emission-Ratio-Tunable $CaZr(PO_4)_2$:Eu Phosphors Synthesized in Air Atmosphere for Potential White Light-Emitting Deep UV LEDs. *J. Mater. Chem. C*. **2014**, *2*, 312-318.

(9) Qian, H.; Zhang, J.; Yin, L. Crystal Structure and Optical Properties of White Light-Emitting $Y_2WO_6:Sm^{3+}$ Phosphor with Excellent Color Rendering. *RSC Advc.* **2013**, *3*, 9029-9034

(10) Meetei, S. D.; Singh, S. D. Hydrothermal Synthesis and White Light Emission of Cubic $ZrO_2:Eu^{3+}$ nanocrystals. *J. Alloys Compd.* **2014**, *587*, 143-147.

(11) Li, L.; Noh, H. M.; Moon, B. K.; Jeong, J. H.; Choi B. C.; Liu X. Tunable White-Light Emission in Single-Phase $Ca_9Gd(VO_4)_7:Tm^{3+}$, Eu^{3+}. *Opt. Mater. Express*. **2014**, *4*, 16-28

(12) Sokolnicki J. Enhanced Luminescence of Tb^{3+} Due to Efficient Energy Trasnfer from Ce^{3+} in a Nanocrystalline $Lu_2Si_2O_7$ Host Lattice. *J. Phys.: Condens. Matter.* **2010**, *22*, 275301.

(13) Sokolnicki, J. Rare Earths (Ce,Eu,Tb) Doped $Y_2Si_2O_7$ Phosphors for White LED. *J. Lumin.* **2013**, *134*, 600-606.

(14) Blasse G.; Grabmaier B.C., Luminescent Materials, Springer Verlag: Berlin, Germany, 1994.

(15) Felsche J. The Crystal Chemistry of the Rare-Earth Silicates. *Struct. Bond.* **1973**, *13*, 99-197.

(16) Li, Y.; Wei, X.; Yin, M.; Tao, Y. Energy Transfer Processes in Ce^{3+} and Tb^{3+} Co-doped $Ln_2Si_2O_7$ (Ln = Y, Gd). *Opt. Mater.* **2011**, *33*, 1239-1242.

(17) Li, Y.; Wang, C.-N.; Wie, X.-T.; Zhao, J.-B.; Zhang, W.-P.; Yin, M. Synthesis and Luminescent Properties of Nanoscale $Gd_2Si_2O_7:Eu^{3+}$ Phosphors. *J. Nanosci. Nanotechnol.* **2010**, *10*, 2219-2222.

(18) Madhukar, R. C.; Dilip, G. R.; Deva, P. R. B. Spectroscopic and Photoluminescence Characteristics of Dy^{3+} Ions in Lead Containing Sodium Fluoroborate Glasses for Laser Materials. *J. Phys. Chem. Solids.* **2011**, *72*, 1436-1441.

(19) Jayasimhadri, M.; Jang, K.; Lee, H. S.; Chen, B.; Yi, S.-S.; Jeong, J.-H. White Light Generation from Dy^{3+}-doped $ZnO-B_2O_3-P_2O_5$ Glasses. *J. Appl. Phys.* **2009**, *106*, 013105-013114.

(20) ICDD PDF-4+; Soorya K., Ed; International Centre for Diffraction Data, Newtown Square, PA, 2011.

(21) TOPAS version 4.2, Bruker AXS, 2009.

(22) Evans, J. S. O. Advanced Input Files and Parametric Quantitative Analysis Using Topas. *Mater. Sci. Forum.* **2010**, *651*, 1-9.

(23) McCamy, C. S. Correlated Color Temperature as an Explicit Function of Chromaticity Coordenates. *Color Res. Appl.* **1992**, *2*, 142-144.

(24) Smolin, Y. J.; Shepelev, Y. F. The Crystal Structures of the Rare Earth Pyrosilicates. *Acta Crystallogr. B.* **1970**, *26*, 484− 664.

(25) Shannon, R. D. Revised Effective Ionic radii and Systematic Studies of Interatomic Distances in Halides and Chalcogenides. *Acta Cryst. A*. **1976**, *32*, 751−767.

(26) Debasu, M. L.; Ananias, D.; Rocha, J.; Malta, O. L.; Carlos, L. D. Energy-Transfer from Gd(III) to Tb(III) in (Gd, Yb, Tb)PO_4 Nanocrystals. *Phys. Chem. Chem. Phys.* **2013**, *15*, 15565-15571.

(27) Han, S.D.; Khatkar, S.P.; Taxak, V.B.; Sharma, G.; Kumar, D. Synthesis, Luminescence and Effect of Heat Treatment on the Properties of Dy^{3+}-doped YVO_4 Phosphor. *Mater. Sci. Eng. B.* **2006**, *129*, 126-130.

(28)Yu, M.; Lin, J.;Wang, Z.; Fu, J.; Wang, S.; Zhang, H. J.; Han, Y. C. Fabrication, Patterning, and Optical Properties Of Nanocrystalline YVO_4:A (A = Eu^{3+}, Dy^{3+}, Sm^{3+}, Er^{3+}) Phosphor Films Via Sol−Gel Soft Lithography**.** *Chem. Mater.* **2002**, *14*, 2224-2231.

(29) Wu, Y.; Wang, Y.; He, D.; Fu, M.; Zhao, Y.; Li, Y.; Miao, F. Synthesis and Luminescence Properties of Sr_2SiO_4:Eu^{3+}, Dy^{3+} Phosphors by the Sol-Gel Method*. J. Nanosci. Nanotech.* **2011**, *11*, 9439-9444.

(30) Zhao, W.; An, S.; Fan, B.; Li, S.; Dai, Y. The VUV‑vis Luminescent Properties of $NaYFPO_4$: Dy^{3+} Phosphor. *J. Lumin*. **2012**, *132*, 953-956.

(31) Su, Q.; Pei, Z.; Chi, L.; Zhang, H.; Zhang, Z.; Zou, F. The Yellow-To-Blue Intensity Ratio (*Y/B*) of Dy^{3+} Emission. *J. Alloys Compd.* **1993**, *192*, 25-27.

(32) Sayed, F. N.; Grover, V.; Dubey, K. A.; Sudarsan, V.; Tyagi, A. K. Solid State White Light Emitting Systems Based on CeF_3: RE^{3+} Nanoparticles and Their Composites with polymers. *J. Colloid Interface Sci.* **2011***, 353,* 445−453.

(33) Jayasimhadri M., Jang K., Lee H. S., Chen B., Yi S.-S., Jeong J.-H. White Light Generation from Dy^{3+}-doped ZnO-B_2O_3-P_2O_5 Glasses. *J. Appl. Phys.* **2009**, *106*, 013105-013114.

(34) Liang, C. H.; Teoh, L. G.; Liu, K. T.; Chang, Y. S. Near White Light Emission of BaY_2ZnO_5 Doped with Dy^{3+} Ions. *J. Alloys Compd.* **2012**, *517*, 9-13.

(35) Xu, Z.; Bian, S.; Wang, J.; Liu, T.; Wang, L.; Gao, Y. Preparation and Luminescence of $La_2O_3:Ln^{3+}$ (Ln^{3+} = Eu^{3+}, Tb^{3+}, Dy^{3+}, Sm^{3+}, Er^{3+}, Ho^{3+}, Tm^{3+}, Yb^{3+}/Er^{3+}, Yb^{3+}/Ho^{3+}) Microspheres. *RSC Adv.* **2013**, *3*, 1410–1419.

(36) Paschotta, R. Encyclopedia of Laser Physics and Technology. Wiley VCH. p. 219. ISBN 978-3-527-40828-3.

(37) Yerpude, A. N.; Dhoble, S. J. Luminescent properties of $Eu^{2+}$and Dy^{3+} ions in $Ba_4Al_2O_7$ phosphor for solid state lighting *J. Lumin.* **2012**, 132, 1781-1785.

(38) Liang, C. H.; Teoh, L. G.; Liu, K. T.; Chang, Y.S. Near white light emission of BaY_2ZnO_5 doped with Dy^{3+} ions. *J. Alloys Comp*. **2012**, *517,* 9-13.

(39) Cao, C.; Yang, H. K.; Moon, B. K.; Choi, B. C.; Jeong, J. H. Host sensitized white luminescence of Dy^{3+}-activated $GdPO_4$ phosphors. *J. Electrochem. Soc.* **2011**, *158*, J6−J9.

[40] Smet, P. F.; Parmentier, A. B.; Poelman, D. Selecting conversion phosphors for white light-amitting diodes. *J. Electrochem. Soc.* **2011**, *158*, R37-R54.

(41) Nazarov, M.; Noh, D.Y.; Sohn, J.; Yoon, C. Influence of Additional Eu^{3+} Coactivator on the Luminescence Properties of $Tb_3Al_5O_{12}:Ce^{3+}$, Eu^{3+}. *Opt. Mater.* **2008**, *30*, 1387-1392.

(42) Jia, P. Y; Lin, J; Han, X. M.; Yu, M. Pechini Sol‑Gel Deposition and Luminescence Properties of $Y_3Al_{5-x}Ga_xO_{12}:Ln^{3+}$ (Ln^{3+}=Eu^{3+}, Ce^{3+}, Tb^{3+}; $0 \le x \le 5$) Thin Films. *Thin Solid Films*. **2005**, *483*, 122-129.

(43) Yong, L.; Baogui, Y.; Weiping, Z.; Min, Y. Luminiscent Properties of β-$Lu_2Si_2O_7:RE^{3+}$ (RE = Ce, Tb) Nanoparticles by Sol-Gel Method. *J. Rare Earths.* **2008**, *26*, 455-458.

(44) Liu, X.; Lin, J. $LaGaO_3$ (A = Sm^{3+} and/or Tb^{3+}) as Promising Phosphors for Field Emission Displays. *J. Mater. Chem.* **2008**, *18*, 221-228.

(45) Pavitra, E.; Raju, G. S. R.; Ko, Y. H.; Yu, J. S. A Novel Strategy for Controlable Emissions from Eu^{3+} or Sm^{3+} Ions co-Doped $SrY_2O_4:Tb^{3+}$ Phosphors. *Phys. Chem. Chem. Phys.* **2012**, *14*, 11296-11304.

(46) Pisarki, W. A.; Zur, L.; Soltys, M.; Pisarka, J. Terbium-Terbium in Lead Phosphate Glasses. *J. Appl. Phys.* **2013**, *113*, 143504.

(47) Rodriguez-Liviano, S.; Aparicio, F. J.; Becerro, A. I.; García-Sevillano, J.; Cantelar, E.; Rivera, S.; Hernández, Y.; De la Fuente, J. M.; Ocaña, M. Synthesis and Functionalization of Biocompatible Tb:$CePO_4$ Nanophosphors with Spindle-Like Shape. *J. Nanopart. Res.* **2012**, *15*, 1402-1407.

(48) Debasu, M. L.; Ananias, D.; Rocha, J.; Malta, O. L.; Carlos, L. D. Energy-Transfer from Gd(III) to Tb(III) in (Gd, Yb, Tb)PO_4 Nanocrystals. *Phys. Chem. Chem. Phys.* **2013**, *15*, 15565-15571.

(49) Nag, A.; Kutty, T. R. N. Photoluminescence Due to Efficient Energy Transfer from Ce^{3+} to Tb^{3+} and Mn^{2+} in $Sr_3Al_{10}SiO_{20}$. *Mater. Chem. Phys.* **2005**, *91*, 524-531.

(50) Hao, Z.; Zhang, J.; Zgang, X.; Lu, S.; Wang, X. Blue-Green-Emitting Phosphor $CaSc_2O_4:Tb^{3+}$: Tunable Luminescence Manipulated by Cross-Relaxation. *J. Electrochem. Soc.* **2009**, *156*, H193-H196.

(51) Sayed, F. N.; Grover, V.; Sudarsan, V.; Pandey, B. N.; Asthana, A.; Vatsa, R. K.; Tyagu, A. J. Multicolored and White Phosphors Based on Doped GdF_3 Nanoparticles and Their Potential Bio-Applications. *J. Colloid Interface Sci.* **2012**, *367*, 161-170.

(52) Lokeswara, R. G. V.; Moorthy, L. R.; Chengaiah, T.; Jamalaiah, B. C. Multi-Color Emission Tenability and Energy Transfer Studies of $YAl_3(BO_3)_4:Eu^{3+}/Tb^{3+}$ Phosphors. *Ceram. Int.* **2014**, *40*, 3399-3410.

(53) Zhang, X.; Zhao, Z.; Zhang, X.; Marathe, A.; Cordes, D.B.; Weeks, B.; Chaudhuri J. Tunable Photoluminescence and Energy Transfer of $YBO_3:Tb^{3+}$, Eu^{3+} for White Light Emitting Diodes. *J. Mater. Chem. C.* **2013**, *1*, 7202-7207.

(54) Sotiriou, G. A.; Schneider, M.; Pratsinis, S. E. Color-Tunable Nanophosphors by Codoping Flame Made Y_2O_3 with Tb^{3+} and Eu^{3+}. *J. Phys. Chem C.* **2011**, *115*, 1084-1089.

(55) Guo, H.; Li, F.; Wei, R.; Zhang, H.; Ma, C. Elaboration and Luminescent Properties of Eu/Tb Co-Doped $GdPO_4$-Based Glass Ceramics for White LEDs. *J. Am. Ceram. Soc.* **2012**, *95*, 1178-1181.

TABLE OF CONTENTS IMAGE